

185  
8-25-81

ORNL MASTER

OR-2971  
B6677

ORNL/TM-7746

OAK  
RIDGE  
NATIONAL  
LABORATORY



### Equilibrium Field Coil Concepts for Intor

D. J. Strickler  
Y-K. M. Peng  
T. G. Brown

OPERATED BY  
UNION CARBIDE CORPORATION  
FOR THE UNITED STATES  
DEPARTMENT OF ENERGY

DISTRIBUTION OF THIS DOCUMENT IS UNLIMITED

ORNL/TM-7746  
Dist. Category UC-20 g

Contract No. W-7405-eng-26

FUSION ENERGY DIVISION

EQUILIBRIUM FIELD COIL CONCEPTS  
FOR INTOR

D. J. Strickler

Computer Sciences Division

Y-K. M. Peng

Fusion Energy Division

T. G. Brown

Grumman Aerospace Corporation  
Bethpage, New York 11714

**NOTICE** This document contains information of a preliminary nature.  
It is subject to revision or correction and therefore does not represent a  
final report.

Date Published - August 1981

Prepared by the  
Oak Ridge National Laboratory  
Oak Ridge, Tennessee 37830  
operated by  
UNION CARBIDE CORPORATION  
for the  
DEPARTMENT OF ENERGY

**DISCLAIMER**  
This document is an account of work sponsored by an agency of the United States Government. Neither the United States Government nor any agency thereof, nor any of their employees, makes any warranty, express or implied, or assumes any legal liability or responsibility for the accuracy, completeness, or usefulness of any information, apparatus, product, or process disclosed, or represents that its use would not infringe privately owned rights. Reference herein to any specific commercial product, process, or service by trade name, trademark, manufacturer, or otherwise, does not necessarily constitute or imply its endorsement, recommendation, or favoring by the United States Government or any agency thereof. The views and opinions of authors expressed herein do not necessarily state or reflect those of the United States Government or any agency thereof.

DISTRIBUTION OF THIS DOCUMENT IS UNLIMITED

## CONTENTS

|                                                                |    |
|----------------------------------------------------------------|----|
| ABSTRACT . . . . .                                             | v  |
| ACKNOWLEDGMENTS . . . . .                                      | 1  |
| 1. INTRODUCTION . . . . .                                      | 3  |
| 2. METHODS . . . . .                                           | 5  |
| 3. EQUILIBRIUM FIELD COIL CONCEPTS . . . . .                   | 7  |
| 3.1 COIL LOCATIONS FOR A SYMMETRIC CONFIGURATION . . . . .     | 7  |
| 3.2 EFFECT OF TRIANGULARITY . . . . .                          | 9  |
| 3.3 HYBRID EF COIL SYSTEM . . . . .                            | 11 |
| 3.4 STEADY-STATE EXTERNAL COILS . . . . .                      | 13 |
| 4. POLOIDAL MAGNETICS OF AN ASYMMETRIC CONFIGURATION . . . . . | 17 |
| 4.1 EXTERNAL EF COILS FOR A SINGLE-NULL PLASMA . . . . .       | 17 |
| 4.2 THE PLASMA SCRAPEOFF REGION . . . . .                      | 17 |
| 4.3 DIVERTOR MAGNETICS OF AN ELLIPTICAL PLASMA . . . . .       | 20 |
| 4.4 STABILITY CONSIDERATIONS . . . . .                         | 20 |
| 4.5 THE DESIGN CONFIGURATION . . . . .                         | 21 |
| 5. CONCLUSIONS . . . . .                                       | 23 |
| REFERENCES . . . . .                                           | 25 |

## ABSTRACT

The following is a summary of work carried out at the Fusion Engineering Design Center at Oak Ridge in the area of equilibrium field (EF) coil design for the International Tokamak Reactor (INTOR). Methods are presented for reducing ampere-turn requirements in the EF coil system. It is shown that coil currents in an EF coil system external to the toroidal field coils can be substantially reduced by relaxing the triangularity of a D-shaped plasma. Further reductions are realized through a hybrid EF coil system using both internal and external coils. Equilibrium field coils for a poloidally asymmetric, single-null INTOR configuration are presented. It is shown that the shape of field lines in the plasma scrapeoff region and divertor channel improves as triangularity is reduced, but it does so at the possible expense of achievable stable beta values.

## ACKNOWLEDGMENTS

The authors would like to thank D. B. Montgomery for suggesting steady-state external coils and Teresa Craig for her careful typing of the report.

## 1. INTRODUCTION

The equilibrium field (EF) coil system in a tokamak device provides the necessary vertical field to position the plasma and to maintain magnetohydrodynamic (MHD) equilibrium. An important requirement of the International Tokamak Reactor (INTOR) EF coil system is to shape the plasma cross section such that a poloidal separatrix is established and its position maintained relative to a divertor channel. It has been shown<sup>1-3</sup> that EF coils external to the toroidal field coils may be found which restrict the movement of the null point to less than 10 cm as beta increases from  $\beta = 0.5\%$  (i.e., prior to heating) to  $\beta > 5.0\%$  (burn). Major engineering problems, however, could be associated with such coil systems. It is well known that ampere-turn requirements increase rapidly as coils are moved further from the plasma. Making these coils superconducting would significantly reduce power requirements, but the size and cost of the poloidal field system may be prohibitive. Further problems caused by large coil currents are the effects of changing poloidal fields at the toroidal field (TF) coils and the large out-of-plane forces on the TF coils created by poloidal fields interacting with the TF coil currents.

The INTOR design under consideration at the Fusion Engineering Design Center (FEDC) in Oak Ridge is a configuration showing vertical asymmetry. The plasma cross section is asymmetric to be consistent with the option of a single-null poloidal divertor. For effective utilization of available space, the midplane of the plasma is above the horizontal centerline of the tokamak, and EF coils are shown in locations that are asymmetric with respect to the plasma.

These characteristics have brought about the need for a numerical computation of vertically asymmetric MHD equilibria that includes an accurate estimate of the necessary EF coil currents. The methods used at the FEDC to study the equilibrium field requirements of double- and single-null divertors are described briefly in Sect. 2.

In Sect. 3 we apply these methods in the study of a symmetrical, double-null poloidal field configuration. We address the possibility of reducing ampere-turns in an INTOR device by relaxing the plasma shaping parameters and introducing some internal coils. The advantages of a hybrid EF coil system and the option of steady-state external coils are discussed.

We consider the magnetics of an asymmetric INTOR configuration in Sect. 4. We present a set of exterior EF coil locations and currents for a plasma of moderate triangularity ( $\delta = 0.3$ ) that fix the position of a single-null point as beta is increased. These coils are positioned to be consistent with the TF coil of a typical design configuration.

A potential problem associated with single-null systems is the shape of field lines in the scrapeoff region of D-shaped plasmas. The direction of field lines on the small major radius side may leave inadequate space for a divertor channel. Furthermore, the proximity of the null point opposite the divertor (above the midplane in current designs) may cause the region to be disconnected. The situation is shown to improve (Sect. 4) if the triangularity is reduced to about  $\delta = 0.1$ , and the implications of this on MHD stability (ballooning modes) are discussed.

## 2. METHODS

To obtain estimates of the EF coil current requirements of an INTOR design configuration, we solve numerically the equation for MHD equilibrium in a tokamak geometry:

$$\Delta^* \Psi = r^2 \nabla \cdot \left( \frac{1}{r^2} \nabla \Psi \right) = -4\pi r J_t \quad , \quad (1)$$

where the poloidal flux function  $\Psi = \Psi(\text{plasma}) + \Psi(\text{external})$  satisfies

$$\Psi(\text{plasma})(r_b, z_b) = \iint_{\Omega} G(r_b, z_b; r, z) J_t[r; \Psi(r, z)] dr dz \quad (2)$$

for  $(r_b, z_b)$  on the boundary of a rectangular region  $\Omega$ . Here,  $G$  is a Green's function giving  $\Psi$  at a point  $(r_b, z_b)$  on the boundary created by a unit current density at  $(r, z)$  in  $\Omega$ . To properly shape the plasma cross section, we determine the coil currents  $c_j$  (for a set of given coil locations) such that the external field satisfies

$$\Psi(\text{external})(r, z; \vec{c}) = \Psi(r_L, 0) - \Psi(\text{plasma})(r, z) \quad (3)$$

for  $(r, z)$  on a prescribed (possibly asymmetric) contour  $\Gamma$  intersecting the plasma midplane at a point  $(r_L, 0)$ .

Since determining the currents  $c_j$  in Eq. (3) is, in general, an ill-posed problem, in practice we solve the associated approximation problem

$$\|\vec{\Psi}(\text{external})(\vec{c}) + \vec{\Psi}(\text{plasma}) - \Psi(r_L, 0)\|^2 + \alpha \|\vec{c}\|^2 = \text{minimum} \quad , \quad (4)$$



where the smoothing parameter  $\alpha$  is the weight given to reducing ampere-turns. We try to choose  $\alpha$  as large as possible but such that the shape of the resulting equilibrium remains acceptable.

The toroidal current density is related to the plasma pressure  $P(\Psi)$  and the toroidal magnetic flux  $F(\Psi) = rB_t$  by

$$J_t = r \frac{dP}{d\Psi} + \frac{F}{4\pi r} \frac{dF}{d\Psi} . \quad (5)$$

Pressure profiles are of the form

$$P = P_0 \frac{e^{-\alpha} [1 + (1-x)\alpha] - e^{-\alpha x}}{\alpha(e^{-\alpha} - 1)} , \quad (6)$$

$$x = \frac{\Psi - \Psi_{\text{axis}}}{\Psi_{\text{edge}} - \Psi_{\text{axis}}} ,$$

and  $F^2(x)$  is represented by a cubic spline function such that  $q(\Psi)$  can be prescribed<sup>4</sup> and  $J_t$  will go continuously to zero at the plasma edge.

### 3. EQUILIBRIUM FIELD COIL CONCEPTS

#### 3.1 COIL LOCATIONS FOR A SYMMETRIC CONFIGURATION

The EF coils provide the vertical field necessary for plasma equilibrium and serve to shape the plasma cross section to the extent that is required for MHD stability. Equilibrium field coils for D-shaped plasmas generally fall into distinct groups depending on their position and the direction of current relative to the plasma current. Equilibrium field coils external to the TF coils would be desirable from a maintenance standpoint, but other engineering considerations may require some internal coils.

A set of typical EF coil locations, listed in Table 1, have been specified so that they are compatible with a symmetric 10-TF coil design configuration with major radius  $R_p = 5.42$  m and minor radius  $a = 1.3$  m. Coils  $I_2$  and  $E_2$  are shaping coils and carry current in the same direction as the plasma current.

**Table 1. Equilibrium field coil locations**

|                | R (m) | Z (m) |                  |
|----------------|-------|-------|------------------|
| I <sub>1</sub> | 3.20  | 0.75  | } internal coils |
| I <sub>2</sub> | 4.55  | 3.30  |                  |
| I <sub>3</sub> | 8.20  | 1.90  |                  |
| E <sub>1</sub> | 1.45  | 1.16  | } external coils |
| E <sub>2</sub> | 4.40  | 6.30  |                  |
| E <sub>3</sub> | 10.52 | 4.57  |                  |

In computing equilibria, the coil locations used are symmetric about the midplane. The prescribed contour of constant poloidal flux,  $\Gamma$ , is chosen to be somewhat inside the plasma boundary in order to create a double-null plasma cross section.

### 3.2 EFFECT OF TRIANGULARITY

It has been seen<sup>2-3</sup> that large shaping currents are needed to produce a low beta and highly D-shaped plasma using external EF coils. The International Tokamak Reactor requires that a separatrix be established prior to heating, resulting in the need for low beta shaping.

By varying the position of  $E_2$  within the constraints of the present design configuration (see Fig. 1), the effect of reduced triangularity  $\delta$  in a low beta ( $\beta = 0.5\%$ ,  $I_p = 4.9$  MA,  $B_t = 5.5$  T) plasma is seen in the external coil currents (see Table 2). The triangularity parameter is defined as  $\delta = c/a$ , where  $c$  is the radial shift of the tip of the D and  $a$  is the minor radius. Reductions in excess of 50% in ampere-turns are possible by relaxing this parameter from  $\delta > 0.5$  to  $\delta = 0.36$ .

Another advantage of lower  $\delta$  is the availability of more space on the inboard side of the torus for a divertor channel. The disadvantage is in theoretically lower stable beta values; the implications of this with respect to a current design will be addressed in Sect. 4.4.

Table 2. The effect of relaxing the triangularity is seen in greatly reduced external EF currents

| $\delta$ | $E_1$ (MA) | $E_2$ (MA) | $E_3$ (MA) | $\Sigma  E_i $ |
|----------|------------|------------|------------|----------------|
| 0.55     | -10.2      | 34.0       | -4.6       | 97.6           |
| 0.43     | -7.3       | 17.7       | -4.7       | 59.4           |
| 0.36     | -6.5       | 9.7        | -5.1       | 42.6           |

### 3.3 HYBRID EF COIL SYSTEM

In this section we consider the possibility of further reductions in ampere-turns by introducing some internal EF coils. In such a hybrid system,<sup>5</sup> by using both external superconducting and internal copper coils, the relative magnitude of the equilibrium field supplied by each coil set would be variable and depend on engineering considerations. As an example of such a system, we make two assumptions: (1) external currents at low beta are set to approximately half their high beta value in order to extend their current rise time, and (2) internal currents are limited to about 1.6 MA to restrict their size. The resulting current requirements are shown in Table 3 for a low beta plasma and in Table 4 for the high beta case.

Another consideration in determining the final contributions of external and internal coils to the required equilibrium field is divertor design and the shape of the poloidal field in the region of the divertor channel. The low beta free-boundary equilibrium calculation using hybrid EF coils is shown in Fig. 2, whereas Figs. 3, 4, and 5 exhibit the high beta equilibria using internal, external, and hybrid coil sets, respectively. These show roughly the range of flux patterns that can be produced in the divertor region with the hybrid EF coil system. Finally, the approximate current waveforms are presented in Fig. 6. Note that the use of hybrid coils reduces the size of the external shaping coil  $E_2$  by 50% and will significantly reduce its required power by extending the current rise time.

Table 3. Coil currents (MA) for a low beta ( $\beta = 0.5\%$ ,  $I_p = 4.9$  MA,  $B_t = 5.5$  T,  $\delta = 0.36$ ) equilibrium using the coil locations of Table 1

|       | Internal           | External | Hybrid |
|-------|--------------------|----------|--------|
| $I_1$ | -0.93              | 0.00     | -0.70  |
| $I_2$ | 1.28               | 0.00     | 0.96   |
| $I_3$ | -1.83              | 0.00     | -1.37  |
| $E_1$ | 0.00               | -6.52    | -1.63  |
| $E_2$ | 0.00               | 9.72     | 2.43   |
| $E_3$ | 0.00               | -5.09    | -1.27  |
|       | Total ampere-turns |          |        |
|       | 8.1                | 42.7     | 16.7   |

Table 4. Coil currents (MA) for a high beta ( $\beta = 5.2\%$ ,  $I_p = 6.1$  MA,  $B_t = 5.5$  T) equilibrium using the coil locations of Table 1

|       | Internal           | External | Hybrid |
|-------|--------------------|----------|--------|
| $I_1$ | -0.49              | 0.00     | -0.25  |
| $I_2$ | 1.58               | 0.00     | 0.79   |
| $I_3$ | -3.28              | 0.00     | -1.64  |
| $E_1$ | 0.00               | -4.17    | -2.09  |
| $E_2$ | 0.00               | 12.18    | 6.09   |
| $E_3$ | 0.00               | -8.29    | -4.15  |
|       | Total ampere-turns |          |        |
|       | 10.7               | 49.3     | 30.0   |

Estimates based on this system show that maximum out-of-plane forces on the TF coils at high beta are reduced from 59 MN/m (external system) to 15 MN/m using the hybrid coils, with a 30% reduction in the average moment about the major axis of the tokamak (~260 MN-m with the hybrid system). The average  $dB^{(ext)}/dt$  at the TF coils (in T/s), which is important for cryostability, is approximately  $B_{\perp}^{(ext)} = 0.18$ ,  $B_{\perp}^{(ext)} = 0.12$  with an all-external system and  $B_{\perp}^{(ext)} = 0.03$ ,  $B_{\perp}^{(ext)} = 0.02$  with the hybrid system, showing a significant reduction. The advantage of this hybrid system over an all-internal EF coil system is in the smaller size of internal coils and a reduction in power losses from about 111 MW to 56 MW.

### 3.4 STEADY-STATE EXTERNAL COILS

An alternative hybrid scenario is one in which the external coil currents are steady state. Such a system would minimize pulsed poloidal fields at the TF coils created by the EF coils. The internal coil currents in this case are found by solving the minimization problem [Eq. (4)] with  $\Psi^{(ext)} = \Psi_R^{(ext)} - \Psi_E^{(ext)}$ , where  $\Psi_R^{(ext)}$  is the required equilibrium field and  $\Psi_E^{(ext)}$  is the field created by the external coils. Note that at time  $t = 0$ ,  $\Psi_R^{(ext)} = 0$ , and the internal coils would carry nonzero currents in order to cancel the flux of the steady-state coils.

An example of this hybrid system is presented in Table 5 where we assume that the high beta EF currents are equivalent to those of the hybrid system in Table 4. The first column ( $\beta = 0.0\%$ ) gives the coil currents necessary for a field that is null prior to startup. Note that this concept requires a polarity change in the internal coils.



The equilibrium flux surfaces at low beta using this system are shown in Fig. 7, and approximate current waveforms are given in Fig. 8.

This concept could be used to eliminate the problems of large power requirements and pulsed fields in an external system by setting the steady-state coil currents equal to their high beta external values in Table 4. Here, the internal coil currents would serve to shield the plasma from part of  $\psi_E^{(ext)}$  at low beta and go to zero at high beta.

Table 5. Coil currents (MA) for equilibria using the hybrid coils of Table 1 with steady-state external coils

|                    | $\beta = 0.0\%$ | $\beta = 0.5\%$ | $\beta = 5.2\%$ |
|--------------------|-----------------|-----------------|-----------------|
| $I_1$              | 0.22            | -0.72           | -0.25           |
| $I_2$              | -0.75           | 0.52            | 0.79            |
| $I_3$              | 1.60            | -0.22           | -1.64           |
| $E_1$              | -2.09           | -2.09           | -2.09           |
| $E_2$              | 6.09            | 6.09            | 6.09            |
| $E_3$              | -4.15           | -4.15           | -4.15           |
| Total ampere-turns |                 |                 |                 |
|                    | 29.8            | 27.6            | 30.0            |

16

#### 4. POLOIDAL MAGNETICS OF AN ASYMMETRIC CONFIGURATION

##### 4.1 EXTERNAL EF COILS FOR A SINGLE-NULL PLASMA

In this section we consider a set of EF coils located external to the TF coils of an INTOR configuration creating a mildly D-shaped ( $\delta = 0.3$ ) equilibrium with major radius  $R_p = 5.2$  and minor radius  $a = 1.3$ . The plasma is vertically asymmetric, as is the case with a single-null poloidal divertor. Such external coil locations would be constrained somewhat by device design and maintenance considerations.

The coil locations are presented in Table 6, together with the required ampere-turns for low beta and high beta equilibria. The coil locations shown here are feasible with respect to the space constraints of a current design configuration but require further optimization. The equilibria are shown in Figs. 9 and 10. In these calculations we have elongated the plasma below the midplane until a natural separatrix defines the plasma boundary. Note that if coil currents are individually controlled, as in Table 6, then the position of the null point is maintained to within 10 cm through a large increase in plasma pressure.

##### 4.2 THE PLASMA SCRAPEOFF REGION

Of particular interest in INTOR poloidal divertor design is the shape of field lines in the plasma scrapeoff region immediately outside the flux surface of the null point. The INTOR design assumes a 5-cm scrapeoff width along the midplane on the large major radius side of the plasma, based partially on Poloidal Divertor Experiment (PDX) results.<sup>6</sup> Divertor design studies<sup>7</sup> show that it is desirable to have a

narrow inner divertor throat ( $\sim 30$  cm) with sufficient length for pumping and shielding requirements. The flux surfaces of high beta equilibria are considerably expanded on the inboard side of the torus, as exhibited in Fig. 10. If we assume this expansion to be about a factor of 3 for INTOR, resulting in a 15-cm scrapeoff width on the inside of the plasma at the midplane, then the width at the divertor channel is somewhat greater, and the direction of the diverted field lines in Fig. 10 is such that there is about 2 m in length available for a divertor channel design within the TF coils.

Figure 10 demonstrates another difficulty with D-shaped single-null systems using external EF coils. Note that the null point above the midplane ( $z > 0$ ) is within the scrapeoff, causing part of the region to be disconnected. The dependence of this property on triangularity is shown in Fig. 11. Here, we have fixed the elongation and triangularity in a high beta INTOR plasma to  $\sigma = 1.85$  and  $\delta = 0.2$  below the midplane and the elongation for  $z > 0$  to  $\sigma = 1.4$ . The triangularity above the midplane is varied from  $\delta = 0.0$  to  $\delta = 0.3$  in a sequence of equilibria. It is seen that for about  $\delta > 0.1$ , the upper null point is sufficiently close to the flux surface of the lower null point that a partial disconnection of the scrapeoff region would result. The extent of this problem depends greatly on the actual width of the scrapeoff, which is still uncertain.<sup>6</sup>

Table 6. Coil locations and currents (MA) for low beta equilibrium ( $\beta = 0.3\%$ ,  $\beta_p = 0.2$ ,  $B_t = 5.5$  T,  $I_p = 5.6$  MA) and high beta equilibrium ( $\beta = 5.0\%$ ,  $\beta_p = 2.6$ ,  $B_t = 5.5$  T,  $I_p = 6.5$  MA)

| R (m) | Z (m) | Low beta           | High beta |
|-------|-------|--------------------|-----------|
| 1.35  | 0.50  | -9.38              | -2.99     |
| 1.35  | 5.30  | 3.33               | 3.94      |
| 3.00  | 6.20  | 5.19               | 5.32      |
| 4.70  | 6.60  | 2.57               | 2.35      |
| 6.50  | 6.50  | -0.14              | 2.36      |
| 8.30  | 5.90  | -0.29              | 4.98      |
| 10.15 | 4.90  | -4.08              | -10.98    |
| 1.35  | -0.50 | -17.55             | -8.26     |
| 6.50  | -7.50 | 6.66               | 7.75      |
| 7.80  | -7.20 | 6.52               | 14.57     |
| 10.50 | -5.30 | -12.27             | -19.53    |
|       |       | Total ampere-turns |           |
|       |       | 68.0               | 83.0      |

### 4.3 DIVERTOR MAGNETICS OF AN ELLIPTICAL PLASMA

One possible solution to the divertor magnetics problem is presented in Fig. 12. The inner divertor leg of this elliptical (i.e.,  $\delta = 0.1$ ) plasma is at such an angle that a channel design seems more feasible, and the scrapeoff region remains connected above the midplane. The width of the inner divertor channel is about 25% smaller than that of the D-shaped plasma in Fig. 10.

There are both physics and engineering difficulties associated with plasmas of low triangularity. Elliptical plasmas require EF coils on the outboard side of the torus that are closer to the midplane than those of a D-shaped cross section. This space is unavailable for EF coils in most design configurations. Another potential problem is in critical beta values for MHD stability, which decrease with plasma triangularity.

### 4.4 STABILITY CONSIDERATIONS

It has been shown<sup>8-9</sup> that through optimization of the safety factor and pressure profiles critical beta values with respect to ballooning modes ( $n = \infty$ ) can be realized in INTOR plasmas that are comparable to those of the symmetric case (i.e.,  $\beta_c^\infty = 5.5\%$ ). In this section we find profiles for a D-shaped plasma with  $\beta_c^\infty = 5.1\%$  and examine the effect of decreasing the triangularity.

Figure 13 shows the pressure, toroidal current density, and safety factor profiles of a moderately asymmetric and strongly D-shaped ( $\delta = 0.5$ ) INTOR equilibrium ( $\beta = 5.1\%$ ) that has been determined to be stable to ballooning modes using the General Atomic BLOON code.<sup>10</sup> For a toroidal field of 5.5 T, the plasma current was increased to

$I_p = 9.3$  MA in order to reduce the safety factor at the plasma surface to  $q_{\text{edge}} = 2.2$ . As triangularity is reduced, the plasma becomes unstable to ballooning modes. The increasing region of instability is shown in Fig. 14.

Through a scaling procedure,<sup>11</sup> approximate critical beta for these equilibria may be computed. For  $\delta = 0.3$  and  $\delta = 0.0$ , the values are about  $\beta_c^\infty = 4.5\%$  and  $\beta_c^\infty = 2.7\%$ , respectively. This indicates that if achievable beta values turn out to be limited by ballooning modes, then a significant reduction may be caused by shaping effects alone in an INTOR geometry. It is not clear whether this could be offset through profile optimization.

#### 4.5 THE DESIGN CONFIGURATION

The INTOR design configuration shows a plasma with major radius  $R_p = 5.28$  m, minor radius  $a = 1.2$  m, and elongation  $\sigma = 1.7$ . The null point defining the plasma boundary is located at  $R = 4.76$  m,  $Z = -2.2$  m. Several INTOR groups have successfully computed equilibria satisfying these parameters.<sup>12-13</sup> In Fig. 15 we present an equilibrium with  $\beta = 5.3\%$ ,  $\beta_p = 2.5$ ,  $I_p = 6.5$  MA, and  $B_t = 5.5$  T, approximating these design requirements. The null point of this equilibrium is located at  $R = 4.69$  m,  $Z = -2.27$  m, about 55 cm higher than that of the equilibrium shown in Fig. 10. The EF coil position and currents, given in Table 7, indicate that this elevation of the null point requires a 40% increase in ampere-turns, using EF coils that are external to the INTOR TF coils. The coil locations are shown relative to the plasma cross section in Fig. 16. Coil sizes are based on an assumed current density of  $1500 \text{ A/cm}^2$ .



Table 7. Equilibrium field coil locations and currents for a high beta equilibrium approximating the requirements of the design configuration

| R (m)              | Z (m) | Current (MA) |
|--------------------|-------|--------------|
| 2.30               | 6.50  | 5.78         |
| 3.80               | 6.50  | 10.75        |
| 5.30               | 6.50  | 8.35         |
| 7.80               | 6.50  | -9.38        |
| 10.20              | 4.90  | -2.20        |
| 1.30               | -0.30 | -4.14        |
| 2.80               | -7.50 | 14.70        |
| 4.30               | -7.50 | 23.36        |
| 5.80               | -7.50 | 14.06        |
| 8.30               | -7.50 | -13.16       |
| 10.50              | -5.30 | -11.38       |
| Total ampere-turns |       |              |
|                    |       | 117.8        |

## 5. CONCLUSIONS

The EF coil concept has a direct impact on the structure, maintenance, and overall cost of the INTOR design and the poloidal divertor configuration. Ampere-turns in an all-external EF coil system can be reduced by 50% if the required triangularity of the plasma is lowered from  $\delta > 0.5$  to about  $\delta = 0.36$ . If the triangularity is lowered to near zero, then outer coils located near the midplane are required, and these locations may not be feasible. Therefore, for a design configuration with all-external coils, a plasma of moderate triangularity is desirable.

If engineering considerations such as out-of-plane forces on the TF coils indicate the need for further reductions, a hybrid concept including both internal and external coils can reduce ampere-turns by another 40%. A variation of the hybrid system in which external coils are steady state would eliminate the problem of large pulsed fields at the TF coils caused by external coil currents. Internal coils greatly increase maintenance problems, but the possible benefits warrant further investigation.

An asymmetric D-shaped plasma with a boundary defined by a single poloidal separatrix can be established and maintained through an increase in beta using external EF coils. Magnetics considerations, however, indicate that there are potential problems with the scrapeoff and divertor regions of such plasmas. Reducing the plasma triangularity to near zero is therefore desirable for poloidal divertor design but may have a negative impact on achievable stable beta values. Here again, a moderate triangularity ( $\delta \sim 0.3$ ) is probably a reasonable

compromise. It appears that greater than 100 megampere-turns are required to produce a plasma shape and null point location that is consistent with the requirements of the design configuration using EF coils external to the TF coils.

## REFERENCES

1. D. J. Strickler and Y-K. M. Peng, "Equilibrium Field Coils for the Engineering Test Facility: Shaping the Plasma Cross-Section," Oak Ridge National Laboratory Report ORNL/TM-7339 (September 1980).
2. M. Okabayashi and J. A. Schmidt, "Magnetic Design of a Poloidal Divertor for INTOR," in INTOR Report INTOR/PHY/8-10 (June 1980).
3. D. J. Strickler and Y-K. M. Peng, "Symmetric ETF Poloidal Field Design with Coupled Coils," ETF Design Center Report ETF-R-80-PS-018 (July 1980).
4. J. A. Holmes, Y-K. M. Peng, and S. J. Lynch, "Evolution of Flux Conserving Tokamak Equilibria with Preprogrammed Cross Sections," J. Comput. Phys. 36, 35-54 (1980).
5. Y-K. M. Peng, D. J. Strickler, and R. A. Dory, "Hybrid Equilibrium Field Coils for the ORNL TNS," Proc. 7th Symp. on Engineering Problems in Fusion Research, Vol. I, p. 186 (1977).
6. J. A. Schmidt, "Poloidal Divertor Loads and Channel Design," U.S. INTOR Report INTOR/PHY/80-19 (October 1980).
7. D. Post et al., "Heat Loads, Helium Enrichment, and Pumping of Poloidal Divertors," U.S. INTOR Report INTOR/PHY/80-22 (October 1980).
8. A. M. M. Todd, J. Manickam, M. Okabayashi, M. S. Chance, R. C. Grimm, J. M. Greene, and J. L. Johnson, "Dependence of Ideal-MHD Kink and Ballooning Modes on Plasma Shape and Profiles in Tokamaks," Nucl. Fusion 19, 743 (1979).
9. A. M. M. Todd, A. E. Miller, R. C. Grimm, M. Okabayashi, and H. E. Dalhed, Jr., "Ideal MHD Stability of Poloidally Asymmetric Equilibria," U.S. INTOR Report INTOR/PHY/80-23 (October 1980).
10. D. Dobrott, D. B. Nelson, J. M. Greene, A. H. Glasser, M. S. Chance, and E. A. Frieman, Phys. Rev. Lett. 39, 943 (1977). We wish to thank R. Moore for providing the code.
11. R. G. Bateman and Y-K. M. Peng, Phys. Rev. Lett. 38, 829 (1977).
12. M. Okabayashi (Princeton Plasma Physics Laboratory), private communication, 1981.
13. K. Lackner (IPP Garching), private communication, 1981.

26

## FIGURE CAPTIONS

Fig. 1. The position of the external shaping coil  $E_2$  is varied under the constraints of the design configuration to study the effect of changing triangularity,  $\delta = c/a$ , on external EF coil currents.

Fig. 2. Low beta ( $\beta = 0.5\%$ ) equilibrium flux surfaces using the hybrid EF coil set.

Fig. 3. High beta ( $\beta = 5.2\%$ ) equilibrium flux surfaces using only the internal coil set.

Fig. 4. High beta ( $\beta = 5.2\%$ ) equilibrium flux surfaces using only the external coil set.

Fig. 5. High beta ( $\beta = 5.2\%$ ) equilibrium flux surfaces using the hybrid EF coil set.

Fig. 6. Reference time behavior of internal ( $I_i$ ), external ( $E_i$ ), and hybrid (dashed) currents in MA.

Fig. 7. Low beta ( $\beta = 0.5\%$ ) equilibrium flux surfaces using the hybrid EF coil set with steady-state external coils.

Fig. 8. Reference time behavior of internal coil currents (MA) when external coils carry the steady-state currents:  $E_1 = -2.09$  MA,  $E_2 = 6.09$  MA,  $E_3 = -4.15$  MA.

Fig. 9. D-shaped INTOR equilibrium with triangularity  $\delta = 0.3$ ,  $\beta = 0.3\%$ ,  $\beta_p = 0.2$ ,  $B_t = 5.5$  T, and  $I_p = 5.6$  MA. The location of the null point is  $R = 4.74$  m,  $Z = -2.89$  m.

Fig. 10. D-shaped INTOR equilibrium with triangularity  $\delta = 0.3$ ,  $\beta = 5.0\%$ ,  $\beta_p = 2.6$ ,  $B_t = 5.5$  T, and  $I_p = 6.5$  MA. The location of the null point is  $R = 4.76$  m,  $Z = -2.82$  m.

Fig. 11. In asymmetric D-shaped equilibria, the upper null point is very close to the flux surface of the lower null point. Depending on the width of the scrapeoff, this may lead to disconnection of the region. Here, the plasma shape below the midplane is fixed and the triangularity above the midplane is (a)  $\delta = 0.0$ , (b)  $\delta = 0.1$ , (c)  $\delta = 0.2$ , and (d)  $\delta = 0.3$ .

Fig. 12. INTOR equilibrium with triangularity  $\delta = 0.1$  and parameters  $\beta = 4.9\%$ ,  $\beta_p = 2.5$ ,  $B_t = 5.5$  T, and  $I_p = 6.5$  MA. Elliptical plasmas have desirable properties for poloidal divertor design.

Fig. 13. (a) Plasma pressure, toroidal current density ( $J_t$ ), and (b) safety factor profiles for INTOR equilibrium with triangularity  $\delta = 0.5$  and  $\beta = 5.1\%$ ,  $\beta_p = 1.3$ ,  $B_t = 5.5$  T,  $I_p = 9.3$  MA,  $q_{edge} = 2.2$  that is MHD stable with respect to ballooning modes.

Fig. 14. Increasing region of instability with respect to ballooning modes as plasma triangularity is changed from (a)  $\delta = 0.5$  to (b)  $\delta = 0.3$ , and to (c)  $\delta = 0.0$ .

Fig. 15. High beta ( $\beta = 5.3\%$ ,  $I_p = 6.5$  MA,  $B_t = 5.5$  T) equilibrium with a shape and separatrix position ( $R = 4.69$  m,  $Z = -2.27$  m) approximating that of the INTOR design configuration.

Fig. 16. Equilibrium field coil locations shown relative to the plasma cross section. The coil sizes are based on an assumed current density of  $1500$  A/cm<sup>2</sup>.

ORNL-DWG 81-2201 FED

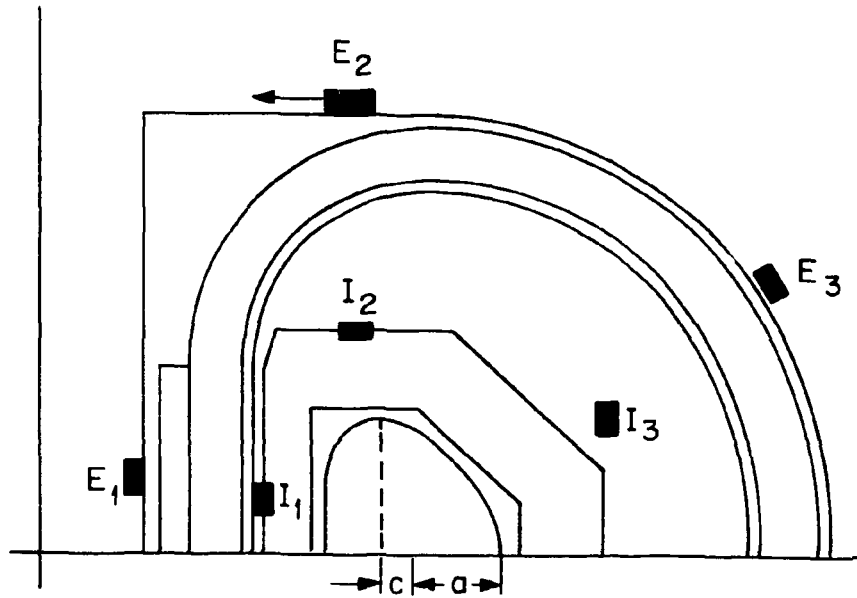


Fig. 1



ORNL-DWG 81-8108 FED

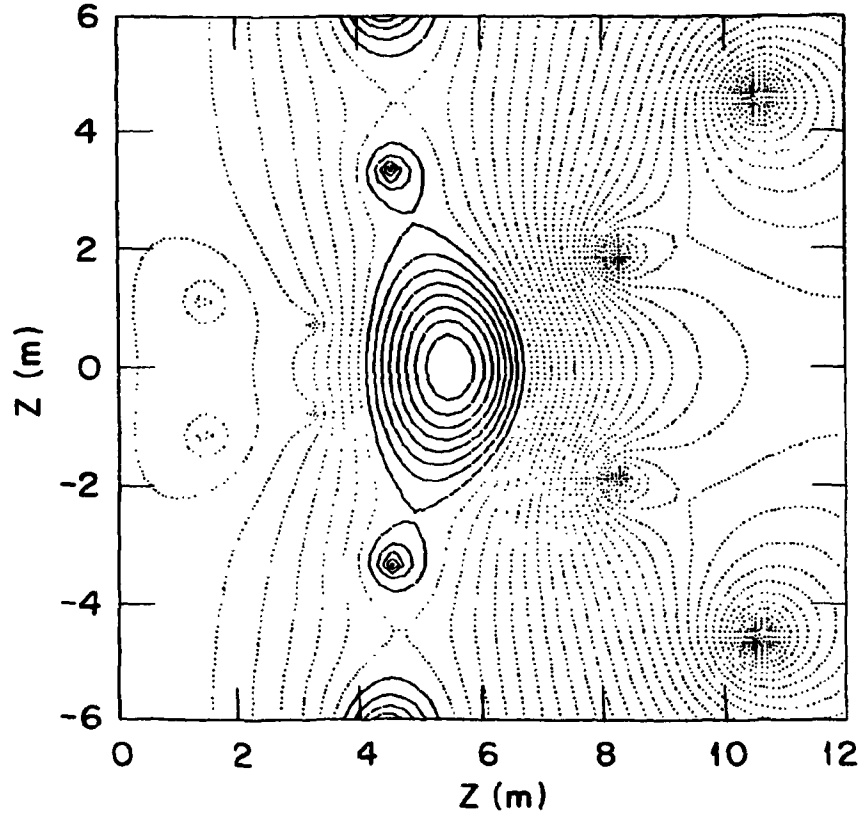


Fig. 2

ORNL-DWG 81-2109 FED

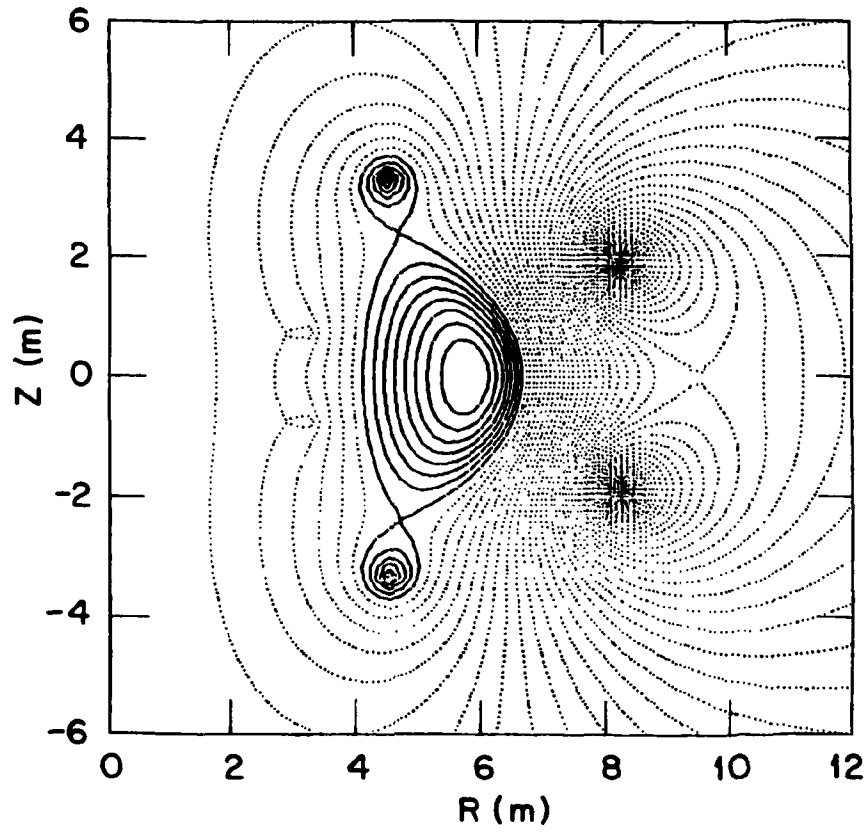


Fig. 3

ORNL-DWG 81-2110 FED

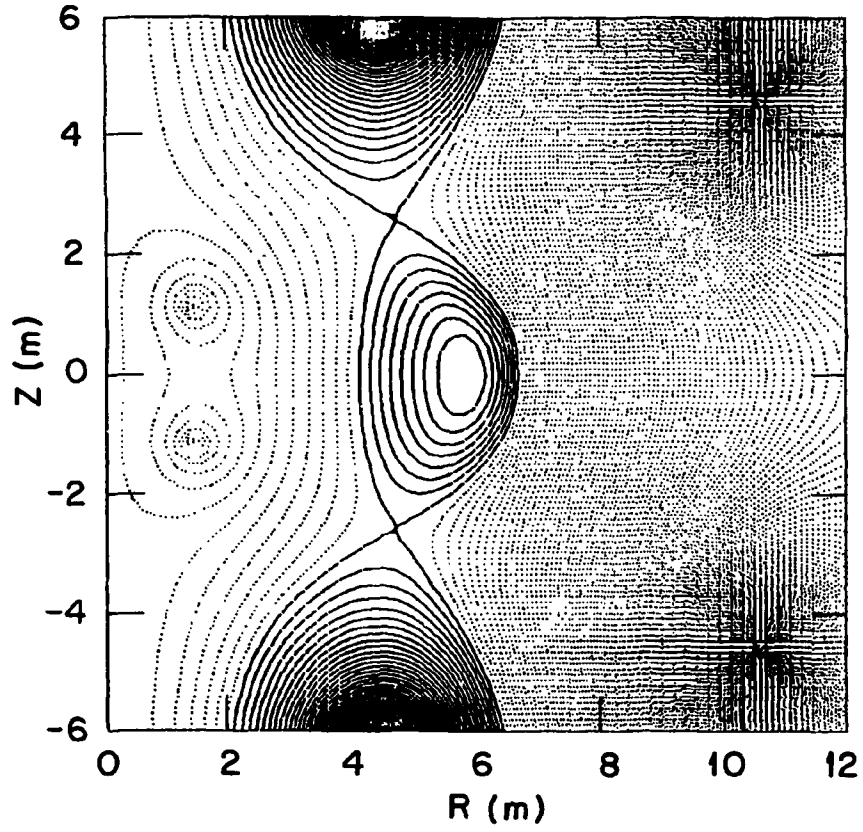


Fig. 4

ORNL-DWG 81-2108 FED

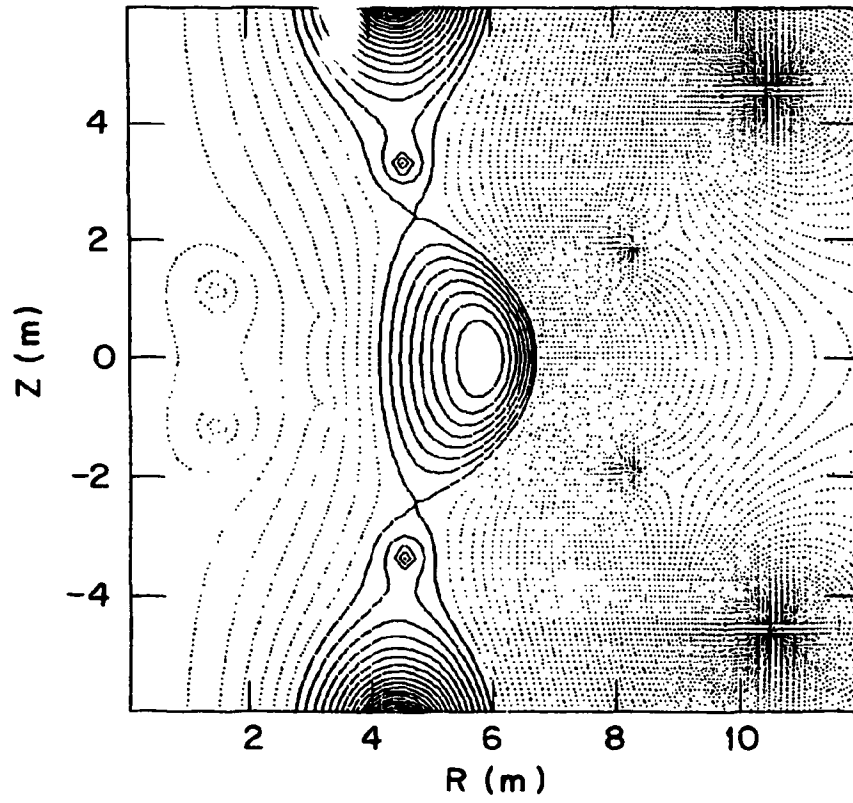


Fig. 5

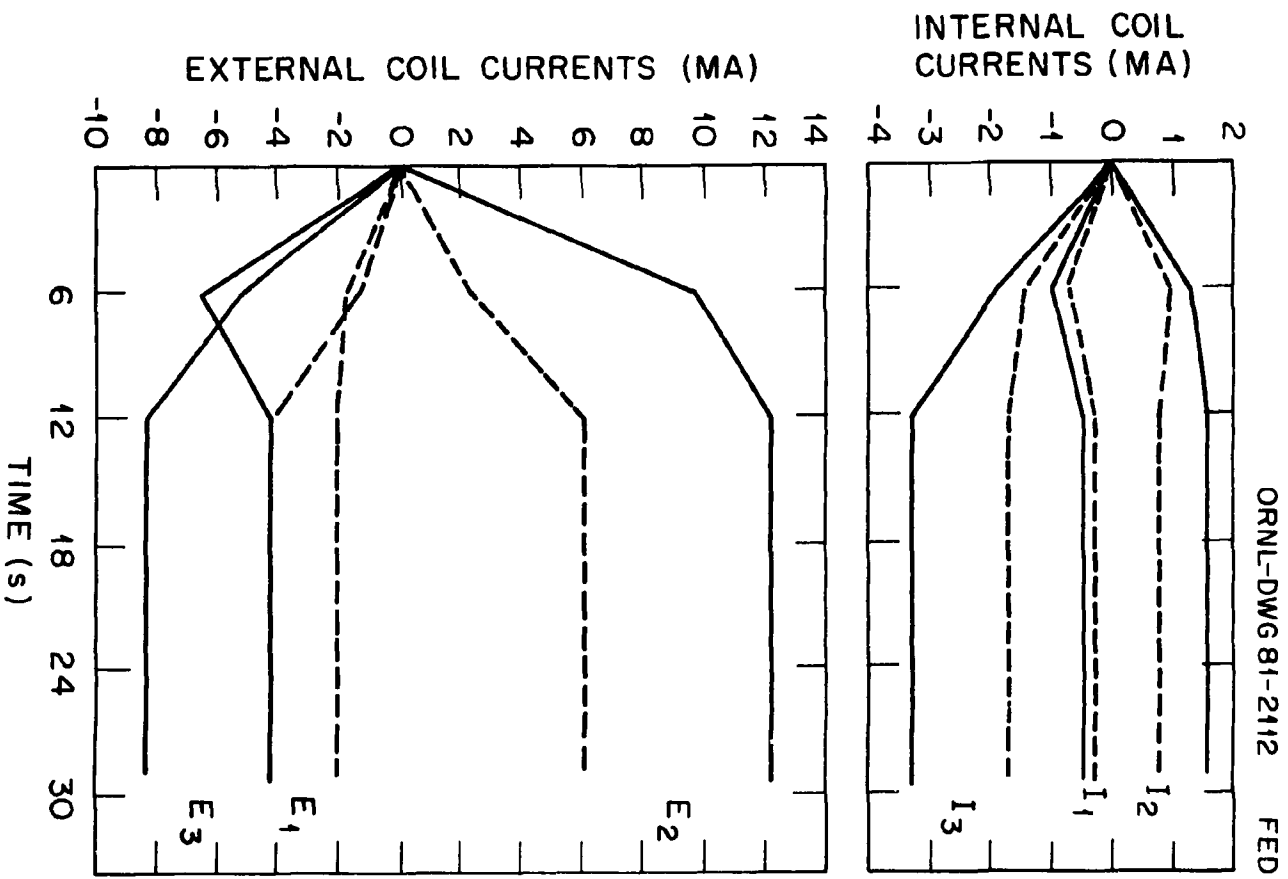


Fig. 6

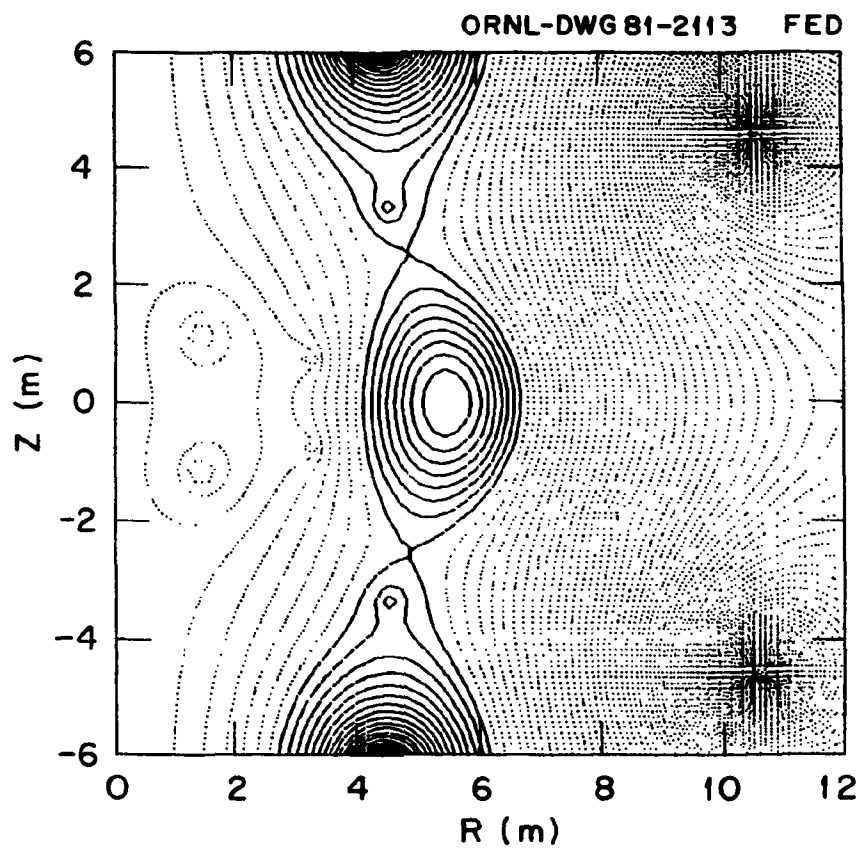


Fig. 7

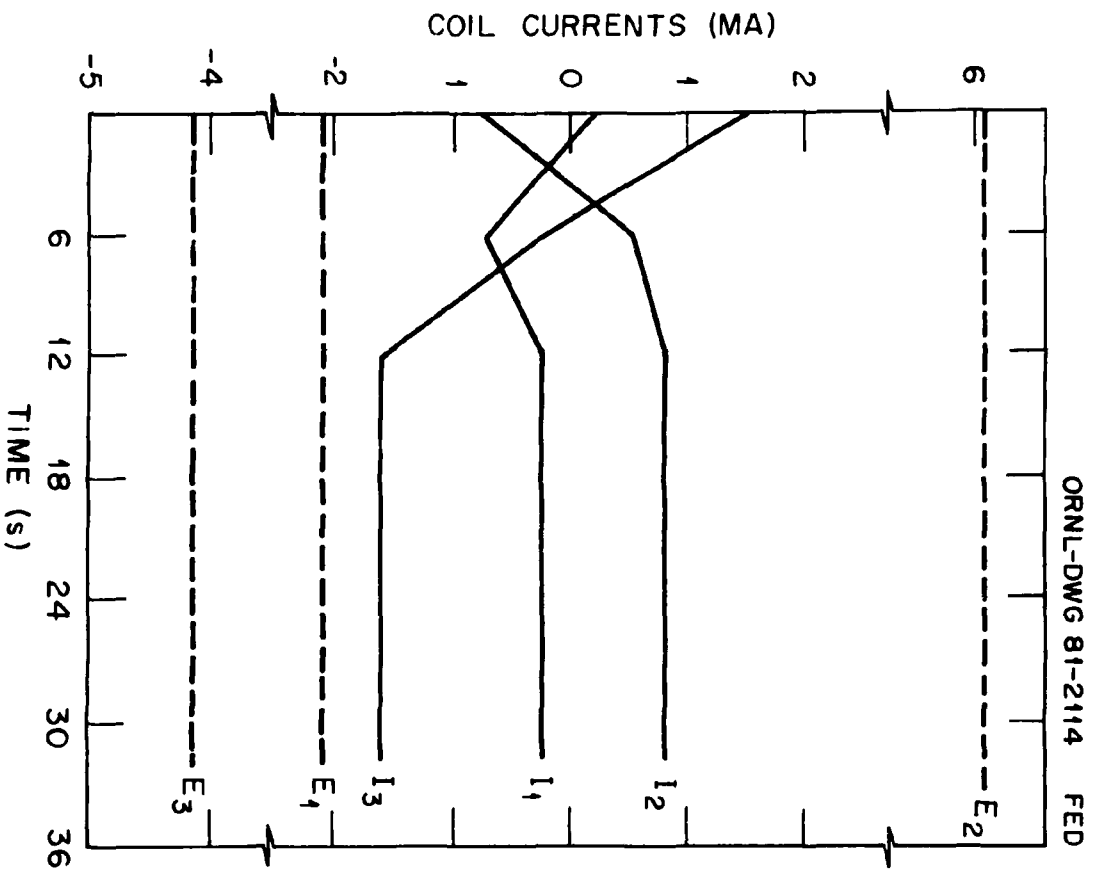


Fig. 8

ORNL-DWG 81-2115 FED

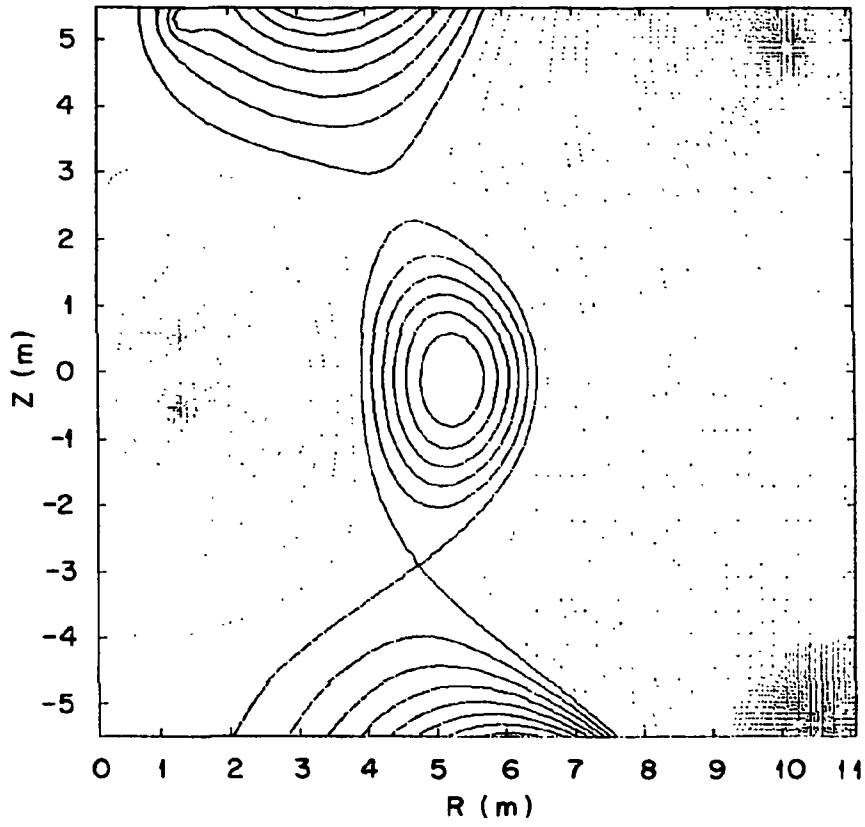


Fig. 9



ORNL-DWG 81-2116R FED

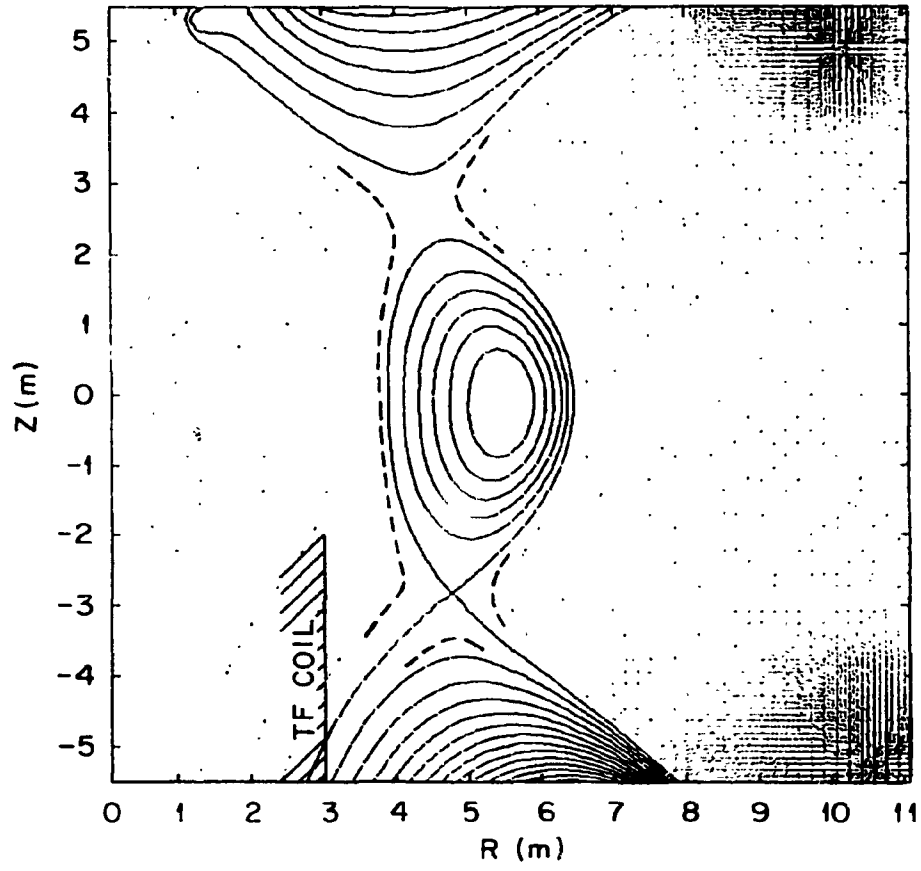


Fig. 10

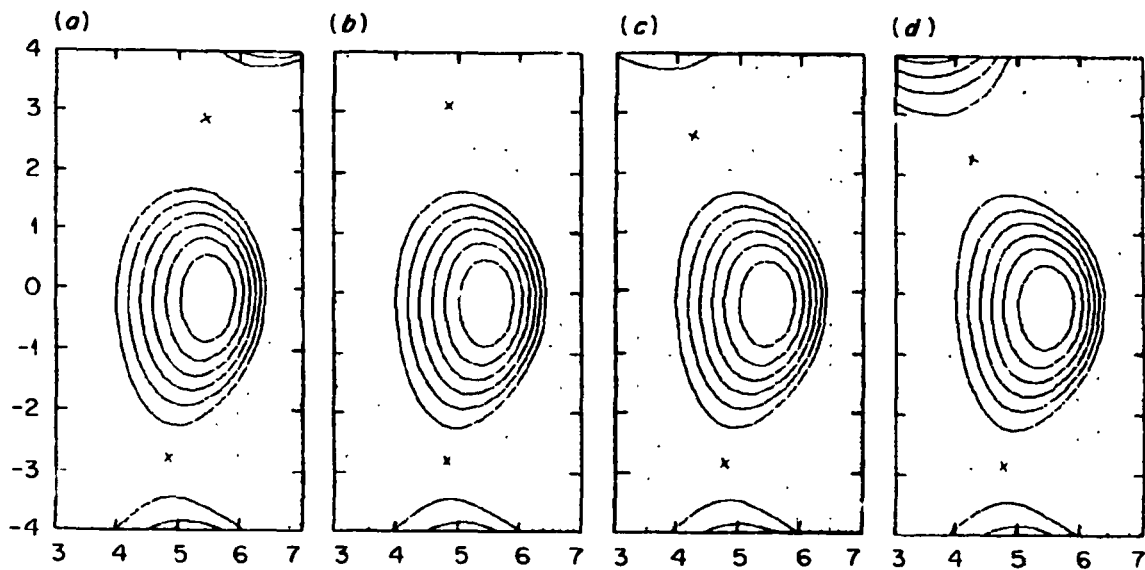


Fig. 11

ORNL-DWG 81-2118R FED

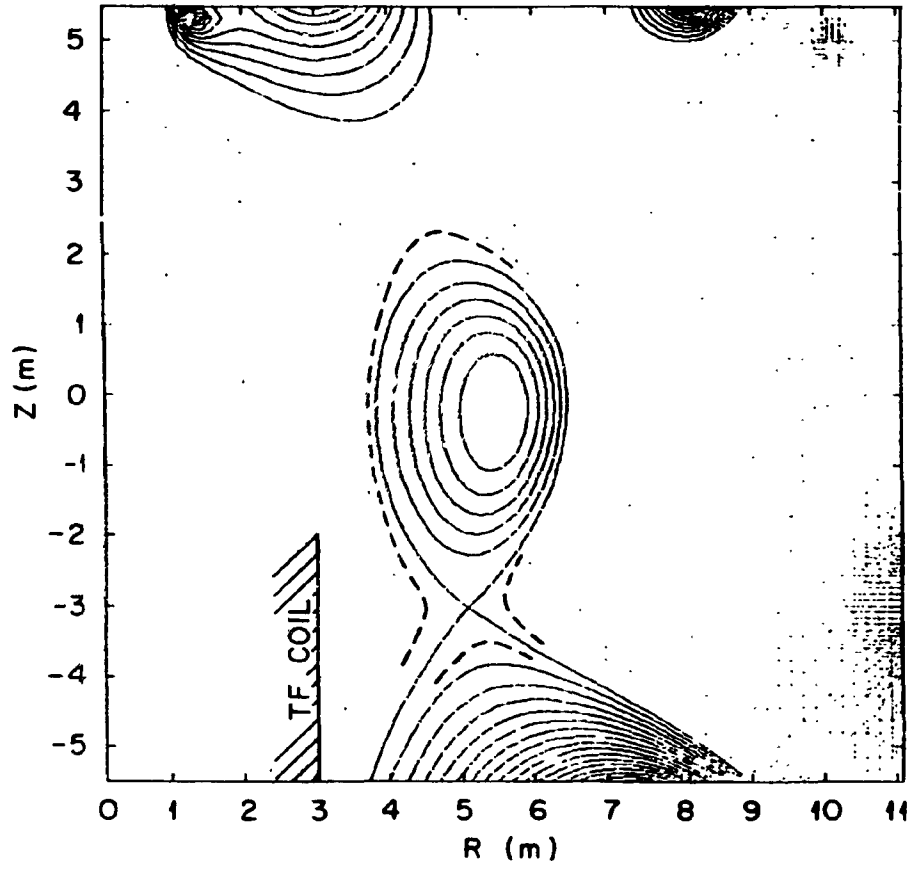


Fig. 12

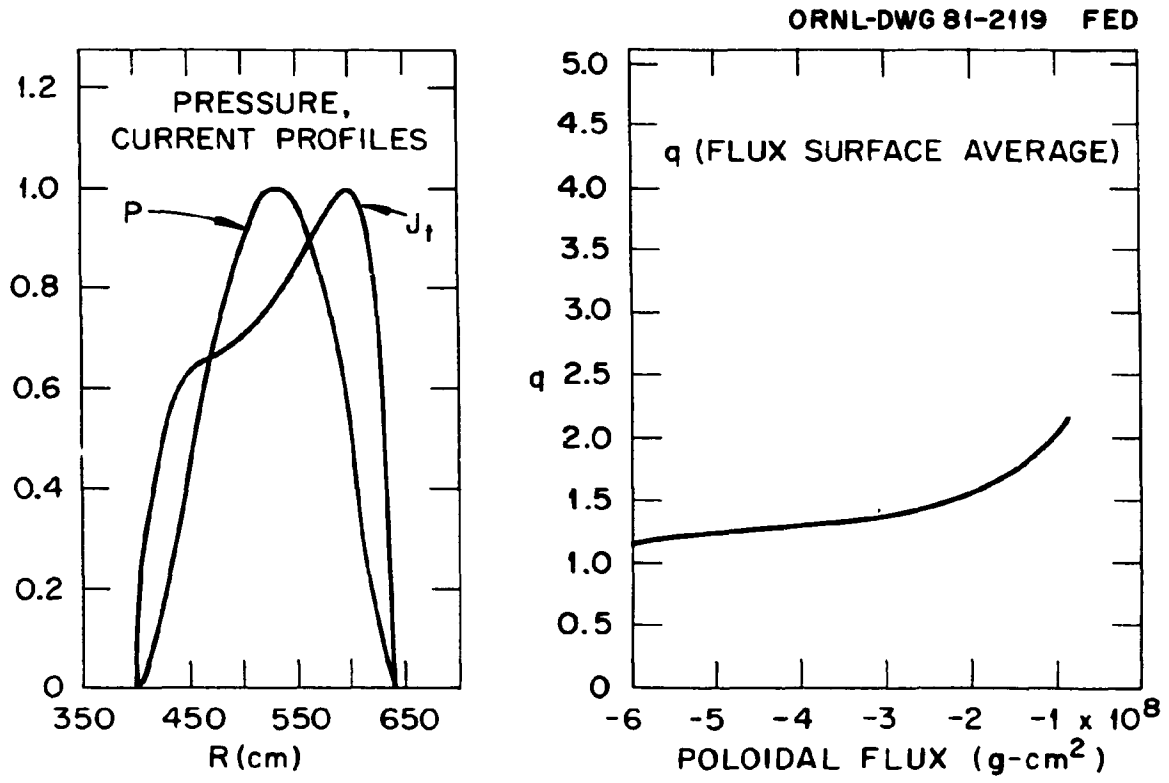


Fig. 13

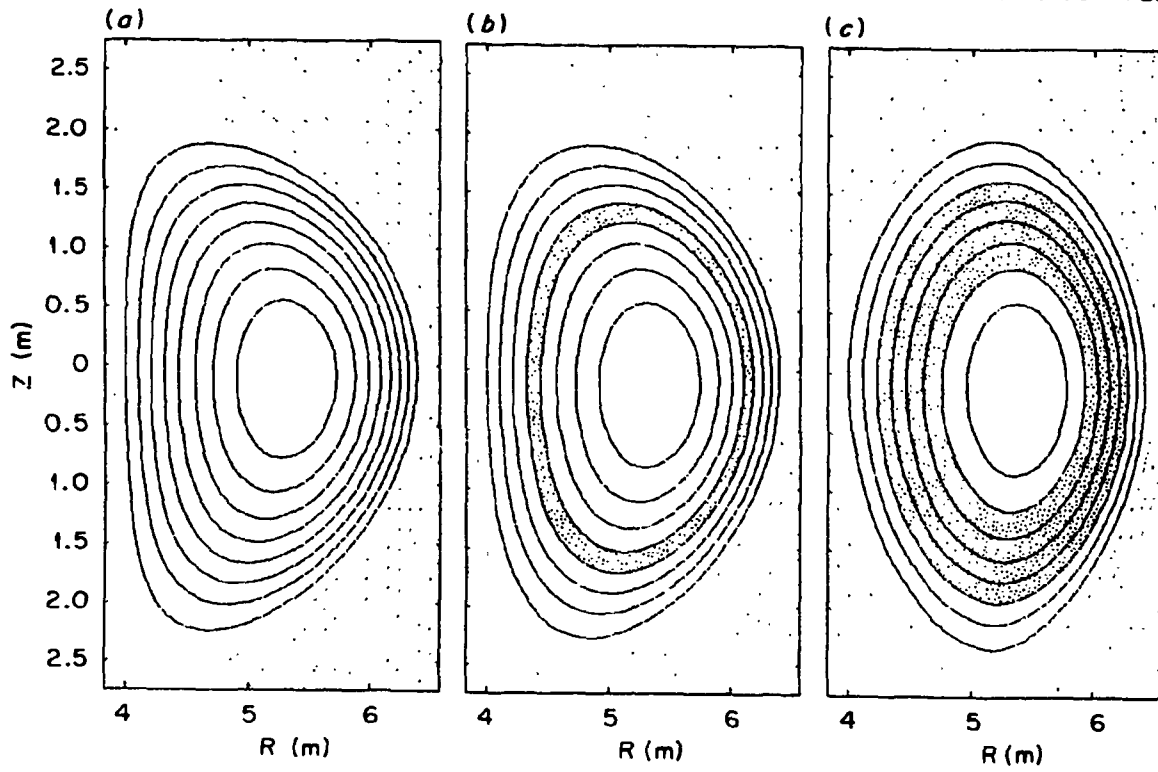


Fig. 14

ORNL-DWG 81-2633 FED

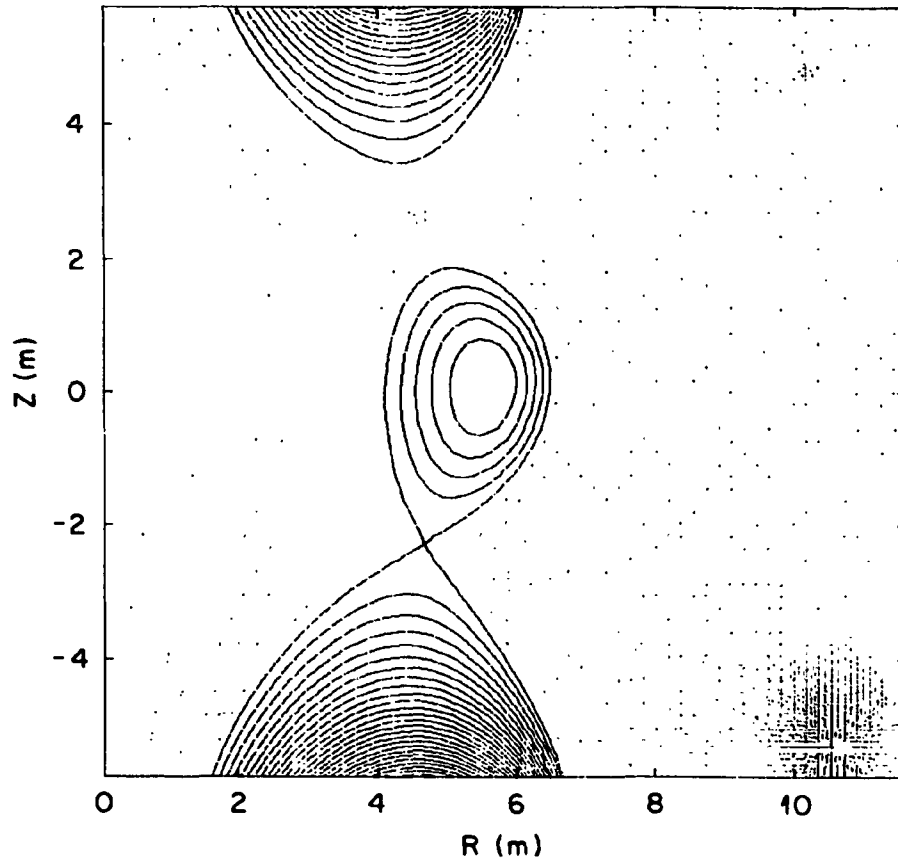


Fig. 15

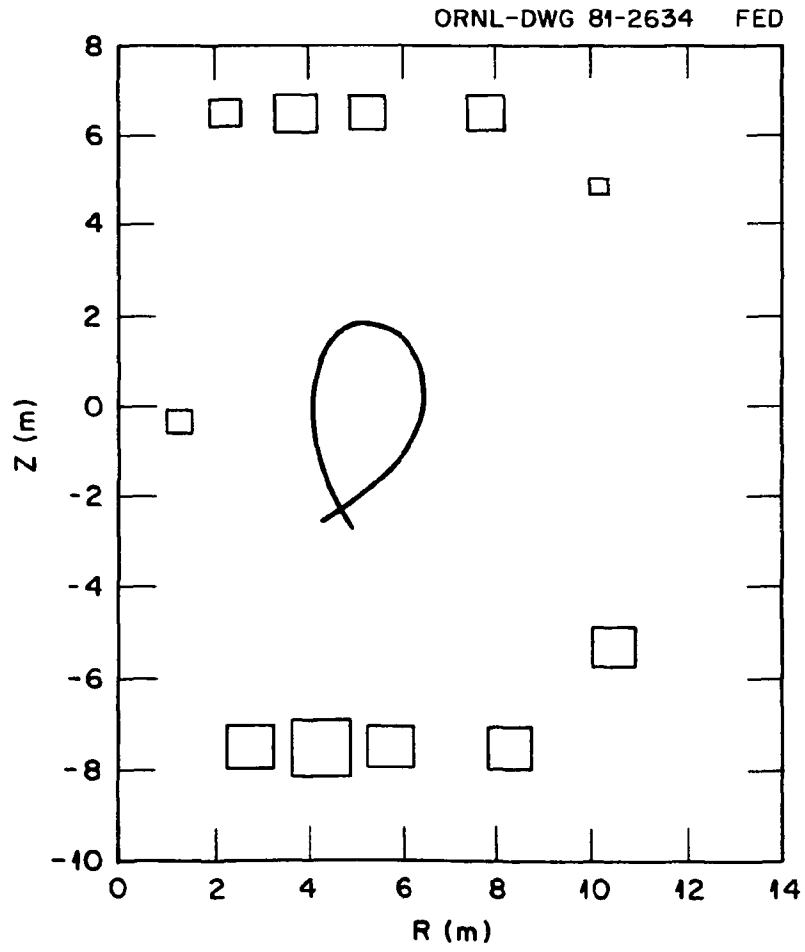


Fig. 16